



Missouri University of Science and Technology
Scholars' Mine

Electrical and Computer Engineering Faculty
Research & Creative Works

Electrical and Computer Engineering

01 Jan 2010

Novel Dynamic Representation and Control of Power Systems with FACTS Devices

Shahab Mehraeen


Jagannathan Sarangapani

Missouri University of Science and Technology, sarangap@mst.edu

Mariesa Crow

Missouri University of Science and Technology, crow@mst.edu

Follow this and additional works at: https://scholarsmine.mst.edu/ele_comeng_facwork

 Part of the [Computer Sciences Commons](#), and the [Electrical and Computer Engineering Commons](#)

Recommended Citation

S. Mehraeen et al., "Novel Dynamic Representation and Control of Power Systems with FACTS Devices," *IEEE Transactions on Power Systems*, vol. 25, no. 3, pp. 1542-1554, Institute of Electrical and Electronics Engineers (IEEE), Jan 2010.

The definitive version is available at <https://doi.org/10.1109/TPWRS.2009.2037634>

This Article - Journal is brought to you for free and open access by Scholars' Mine. It has been accepted for inclusion in Electrical and Computer Engineering Faculty Research & Creative Works by an authorized administrator of Scholars' Mine. This work is protected by U. S. Copyright Law. Unauthorized use including reproduction for redistribution requires the permission of the copyright holder. For more information, please contact scholarsmine@mst.edu.

Novel Dynamic Representation and Control of Power Systems With FACTS Devices

Shahab Mehraeen, *Student Member, IEEE*, S. Jagannathan, *Senior Member, IEEE*, and Mariesa L. Crow, *Fellow, IEEE*

Abstract—FACTS devices have been shown to be useful in damping power system oscillations. However, in large power systems, the FACTS control design is complex due to the combination of differential and algebraic equations required to model the power system. In this paper, a new method to generate a nonlinear dynamic representation of the power network is introduced to enable more sophisticated control design. Once the new representation is obtained, a back stepping methodology for the UPFC is utilized to mitigate the generator oscillations. Finally, the neural network approximation property is utilized to relax the need for knowledge of the power system topology and to approximate the nonlinear uncertainties. The net result is a power system representation that can be used for the design of an enhanced FACTS control scheme. Simulation results are given to validate the theoretical conjectures.

Index Terms—FACTS, neural networks, nonlinear systems, power system control.

I. INTRODUCTION

POWER system stability is defined as the ability of an electric power system, for a given initial operating condition, to regain a state of operating equilibrium after being subjected to a physical disturbance [1]. Power system stability can be improved through the use of dynamic controllers such as power system stabilizers, excitation systems, and more recently FACTS devices. To effectively design the controller, proper modeling of the generators, controller dynamics, and the network must be utilized. A power system is usually modeled using a combination of differential and algebraic equations. The differential equations represent generator angles and speeds whereas the algebraic equations represent bus active and reactive power balance relationships. Incorporating the differential-algebraic equations into the control process is difficult and is made more complex by the inclusion of FACTS devices such as the unified power flow controller (UPFC).

Advanced controller design usually requires that a system be represented by purely differential equations. However, power systems with embedded FACTS devices typically require the algebraic transmission network power balance equations to be included in the system model and it is not straightforward to develop an algebraic equation free system model representation for control purposes.

Manuscript received February 09, 2009; revised September 13, 2009. First published January 26, 2010; current version published July 21, 2010. This work was supported in part by NSF ECCS#0624644. Paper no. TPWRS-00062-2009.

The authors are with the Department of Electrical and Computer Engineering, Missouri University of Science and Technology, Rolla, MO 65409 USA (e-mail: sm347@mst.edu).

Digital Object Identifier 10.1109/TPWRS.2009.2037634

Several approaches have been analyzed for system wide FACTS control design. Past work [2]–[6] has proposed to linearize the differential-algebraic equation network and eliminate the algebraic equations through reduction methods. Then, linear control methods are applied to the linearized power system. This approach, however, tacitly assumes that the network variables remain in the neighborhood of the desired operating point. In addition, the placement and number of UPFC devices are determined heuristically. By contrast, in [7]–[12] a single-machine infinite bus model is used to apply nonlinear control schemes. However, the infinite bus assumption required for this approach is not valid for large multi-machine systems when the fault affects the power system.

FACTS devices have been considered in [13]–[16] via utilizing energy functions to develop the controllers and estimate the critical clearing time. This approach is not practical for controller development because it requires the calculation of the derivatives of power system bus voltages and angles and requires numerical differentiators or approximations. Nonlinear control of a multi-machine power system excitation and governor control has been proposed using back stepping in [17]. This method holds considerable potential, but does not consider FACTS devices. FACTS devices can serve many control functions in an electric power system including steady-state power flow, voltage regulation, and oscillation damping control. Thus, stabilizing capabilities can be added with the other control capabilities without any additional cost. This property is exploited in this work.

In this paper, we propose the following contributions to overcome the above-mentioned challenges:

- 1) A new nonlinear dynamical representation of a power network free of algebraic equations with UPFC as a controller is introduced. This representation is appropriate to model a nonlinear power network with several FACTS devices.
- 2) Oscillation damping is achieved using nonlinear control schemes for UPFCs.
- 3) A neural network approximation property is utilized to relax the need for knowledge of the power system topology and to approximate the nonlinear uncertainties.

Our approach involves first obtaining a nonlinear dynamical representation using network power balance equations. The advantage of this approach is that no algebraic equations are involved in the control design while the nonlinear behavior is retained. In the proposed approach, we use the power system classical model in which the internal voltages of the generators are held constant in order to develop the control design. However, the proposed approach can be extended to more complex generator models without loss of generality. Subsequently, a non-

linear control scheme is developed to stabilize and damp the oscillations resulting from a disturbance such as a three-phase to ground fault. Finally, we have employed the universal approximation property of neural networks (NN) to approximate the power system uncertainties and to relax the need for *a priori* knowledge of the system uncertainties.

II. POWER SYSTEM DIFFERENTIAL-ALGEBRAIC MODEL

The classical generator representation is often sufficient for the control development in order to mitigate the inter-area oscillations since only the rotor speed deviations are of interest. In addition, the resistances of power network lines are neglected. Despite this assumption made for ease of control development, the proposed control will be validated on a full nonlinear power system model.

It is more convenient to represent the generator dynamical equations in the center of inertia (COI) coordinates:

$$\begin{aligned} \dot{\delta}_i &= \omega_i \\ M_i \dot{\omega}_i &= P_{mi} - \frac{M_i}{M_T} P_{COI} \\ &\quad - B_{i,i+n} E_{gi} V_{i+n} \sin(\delta_i - \psi_{i+n}); \quad i = 1, \dots, n \end{aligned} \quad (1)$$

where $\delta_i = \bar{\delta}_i - \delta_0$, $\omega_i = \bar{\omega}_i - \omega_0$, $\psi_i = \bar{\psi}_i - \delta_0$, $M_T = \sum_{i=1}^n M_i$, $\delta_0 = 1/M_T \sum_{i=1}^n M_i \bar{\delta}_i$, $\omega_0 = 1/M_T \sum_{i=1}^n M_i \bar{\omega}_i$, $P_{COI} = \sum_{i=1}^n P_{mi} - \sum_{i=n+1}^{n+N} P_{Li}$ where P_{Li} is the active load at each bus and P_{mi} is the input mechanical power. Also, $\bar{\delta}_i$ is the rotor angle of the i th machine, $\bar{\omega}_i$ is the angular speed, δ_0 is the center of angle, ω_0 is the center of angular speed, B represents the reactance of the admittance matrix, E_{gi} is the i th machine internal voltage, n is the number of generators, $M_i = 2H/\omega_0$ is the i th machine inertia, and V_{i+n} and $\bar{\psi}_{i+n}$ are the generator bus voltage and phase angle, respectively. In addition, N is the number of non-generator buses in the power system.

The bus voltages and phase angles of all of the power system buses are constrained by the following set of algebraic power balance equations (neglecting resistances)

$$\begin{aligned} P_{Li} + \sum_{j=1}^{N+n} B_{ij} V_i V_j \sin(\psi_i - \psi_j) \\ &= S_{Pi} = 0 \\ -Q_{Li} + \sum_{j=1}^{N+n} B_{ij} V_i V_j \cos(\psi_i - \psi_j) \\ &= S_{Qi} = 0; \quad i = n+1, \dots, n+N \end{aligned} \quad (3)$$

where P_{Li} and Q_{Li} are the active and reactive loads on the i th bus and $V_j = E_{gj}$; $\psi_j = \delta_j$ for $1 \leq j \leq n$.

III. NEW DYNAMIC REPRESENTATION OF POWER NETWORKS

Equations (1)–(3) form the set of power system differential-algebraic equations. However, a controller design in a differential-algebraic environment is difficult to achieve, therefore it is desirable to substitute the set of (3) with a more appropriate set.

One way to have a pure dynamical system is to take derivative of (3) to obtain \dot{V}_i and $\dot{\psi}_i$ terms. Thus, we have

$$\begin{aligned} \partial S_{Pi}/\partial t &= \partial S_{Pi}/\partial V \cdot \dot{V} \\ &\quad + \partial S_{Pi}/\partial \psi \cdot \dot{\psi} + \partial S_{Pi}/\partial \delta \cdot \dot{\delta} = 0 \quad (4) \\ &\quad \text{and} \\ \partial S_{Qi}/\partial t &= \partial S_{Qi}/\partial V \cdot \dot{V} \\ &\quad + \partial S_{Qi}/\partial \psi \cdot \dot{\psi} + \partial S_{Qi}/\partial \delta \cdot \dot{\delta} = 0 \\ &\quad i = n+1, \dots, n+N. \end{aligned} \quad (5)$$

Solving (4) and (5) for \dot{V}_i and $\dot{\psi}_i$, we obtain a new set of dynamic equations as

$$\begin{bmatrix} \dot{V} \\ \dot{\psi} \end{bmatrix} = - \begin{bmatrix} \bar{A}(x_S) & \bar{B}(x_S) \\ \bar{D}(x_S) & \bar{E}(x_S) \end{bmatrix}^{-1} \begin{bmatrix} C(x_S) \\ F(x_S) \end{bmatrix} \omega \quad (6)$$

where $V = [V_{n+1} \ V_{n+2} \ \dots \ V_{n+N}]^T$, $\psi = [\psi_{n+1} \ \psi_{n+2} \ \dots \ \psi_{n+N}]^T$, and $\omega = [\omega_1 \ \omega_2 \ \dots \ \omega_n]^T$. Also, we define $\delta = [\delta_1 \ \delta_2 \ \dots \ \delta_n]^T$ and $x_S = [\delta^T \ \omega^T \ V^T \ \psi^T]^T$. Assuming P_{Li} and Q_{Li} to be functions of V_i and ψ_i , we get $\bar{A}_{N \times N} = \partial S_P/\partial V$, $\bar{B}_{N \times N} = \partial S_P/\partial \psi$, $C_{N \times n} = \partial S_P/\partial \delta$, $\bar{D}_{N \times N} = \partial S_Q/\partial V$, $\bar{E}_{N \times N} = \partial S_Q/\partial \psi$, and $F_{N \times n} = \partial S_Q/\partial \delta$ as given in (A3a)–(A4e) in Appendix A. Once again, it is important to note that this step is for controller development and is not required for actual (practical) implementation. The proposed approach is a complementary way of solving the differential-algebraic equations $\{\dot{x} = f(x, z); g(x, z) = 0\}$ where $z = h(x)$ is obtained by solving $g(x, z) = 0$ and replaced in the differential equations $\dot{x} = f(x, z)$ where x is the states of the power system. Solving the nonlinear algebraic equations $g(x, z) = 0$ is a huge challenge (if not impossible in large-scale power systems) which is relaxed in the proposed approach without losing the nonlinear characteristics of the power system.

IV. UPFC AS A NONLINEAR CONTROLLER

In the proposed effort, the UPFC is chosen as a FACTS device which acts as a controller to mitigate system oscillations. The method, however, is applicable to other FACTS devices since the proposed approach is generic and deals with power balance equations as well as generator dynamics. As illustrated in Fig. 1(a), the UPFC shunt transformer is connected to bus $t+n$ and the series transformer is connected between buses $t+n$ and $h+n$. The effect of the UPFC on the power system can be represented as injected powers to the connecting buses [18] as shown in Fig. 1(b). This is referred to as the “power injection” model of the UPFC [18].

The injected active and reactive powers are given by

$$\begin{aligned} P_{t+n} &= B_{t+n, h+n} V_b V_{h+n} \sin(\psi_{t+n} - \psi_{h+n} + \theta) \\ P_{h+n} &= -B_{t+n, h+n} V_b V_{h+n} \sin(\psi_{t+n} - \psi_{h+n} + \theta) \\ Q_{t+n} &= B_{t+n, h+n} V_b V_{t+n} \cos(\theta) \\ Q_{h+n} &= -B_{t+n, h+n} V_b V_{h+n} \cos(\psi_{t+n} - \psi_{h+n} + \theta) \end{aligned} \quad (7)$$

where $\bar{V}_b = V_b \angle(\psi_{t+n} + \theta)$ is the voltage produced by the series transformer and can be assumed to be a function of time. Thus, the power flow equation at buses $t+n$ and $h+n$ can be represented as

$$\begin{aligned} P_{\text{OLD}t+n} + B_{t+n,h+n}V_{h+n}[\gamma \sin(\psi_{t+n} - \psi_{h+n}) \\ + \mu \cos(\psi_{t+n} - \psi_{h+n})] &= 0 \\ P_{\text{OLD}h+n} - B_{t+n,h+n}V_{h+n}[\gamma \sin(\psi_{t+n} - \psi_{h+n}) \\ + \mu \cos(\psi_{t+n} - \psi_{h+n})] &= 0 \\ Q_{\text{OLD}t+n} - B_{t+n,h+n}V_{t+n}\gamma &= 0 \\ Q_{\text{OLD}h+n} + B_{t+n,h+n}V_{h+n}[\gamma \cos(\psi_{t+n} - \psi_{h+n}) \\ - \mu \sin(\psi_{t+n} - \psi_{h+n})] &= 0 \end{aligned} \quad (8)$$

where $\gamma = V_b \cos \theta$, $\mu = V_b \sin \theta$, and P_{OLD} and Q_{OLD} represent the left-hand side of (3). By taking the derivative of (8), (4) and (5) must be modified on the buses $t+n$ and $h+n$. Therefore, considering (4) at bus $t+n$, we get

$$\begin{aligned} \dot{P}_{\text{OLD}t+n} + B_{t+n,h+n}[\gamma \sin(\psi_{t+n} - \psi_{h+n}) \\ + \mu \cos(\psi_{t+n} - \psi_{h+n})]\dot{V}_{h+n} \\ + B_{t+n,h+n}V_{h+n}[\gamma \cos(\psi_{t+n} - \psi_{h+n}) \\ - \mu \sin(\psi_{t+n} - \psi_{h+n})](\dot{\psi}_{t+n} - \dot{\psi}_{h+n}) \\ + B_{t+n,h+n}V_{h+n}[\dot{\gamma} \sin(\psi_{t+n} - \psi_{h+n}) \\ + \dot{\mu} \cos(\psi_{t+n} - \psi_{h+n})] &= 0 \end{aligned} \quad (9a)$$

and at bus $h+n$, we get

$$\begin{aligned} \dot{P}_{\text{OLD}h+n} - B_{t+n,h+n}[\gamma \sin(\psi_{t+n} - \psi_{h+n}) \\ + \mu \cos(\psi_{t+n} - \psi_{h+n})]\dot{V}_{h+n} \\ - B_{t+n,h+n}V_{h+n}[\gamma \cos(\psi_{t+n} - \psi_{h+n}) \\ - \mu \sin(\psi_{t+n} - \psi_{h+n})](\dot{\psi}_{t+n} - \dot{\psi}_{h+n}) \\ - B_{t+n,h+n}V_{h+n}[\dot{\gamma} \sin(\psi_{t+n} - \psi_{h+n}) \\ + \dot{\mu} \cos(\psi_{t+n} - \psi_{h+n})] &= 0. \end{aligned} \quad (9b)$$

Similarly, terms are also added to the left-hand side of (5) at buses $t+n$ and $h+n$ to achieve

$$\dot{Q}_{\text{OLD}t+n} - B_{t+n,h+n}\gamma\dot{V}_{t+n} - B_{t+n,h+n}V_{t+n}\dot{\gamma} = 0 \quad (10a)$$

and

$$\begin{aligned} \dot{Q}_{\text{OLD}h+n} + B_{t+n,h+n}[\gamma \cos(\psi_{t+n} - \psi_{h+n}) \\ - \mu \sin(\psi_{t+n} - \psi_{h+n})]\dot{V}_{h+n} \\ + B_{t+n,h+n}V_{h+n}[-\gamma \sin(\psi_{t+n} - \psi_{h+n}) \\ - \mu \cos(\psi_{t+n} - \psi_{h+n})](\dot{\psi}_{t+n} - \dot{\psi}_{h+n}) \\ + B_{t+n,h+n}V_{h+n}[\dot{\gamma} \cos(\psi_{t+n} - \psi_{h+n}) \\ - \dot{\mu} \sin(\psi_{t+n} - \psi_{h+n})] &= 0. \end{aligned} \quad (10b)$$

By updating matrices \bar{A} , \bar{B} , \bar{D} , and \bar{E} with the additional terms, new matrices A , B , D , and E are obtained and given by (A5a)–(A5d) in Appendix A. Note that matrices C and F remain unchanged. Consequently, (6) becomes

$$\begin{bmatrix} A(x) & B(x) \\ D(x) & E(x) \end{bmatrix} \begin{bmatrix} \dot{V} \\ \dot{\psi} \end{bmatrix} = - \begin{bmatrix} C(x) \\ F(x) \end{bmatrix} \omega - G(x) \quad (11)$$

where $x = [x_S^T \ \gamma \ \mu]^T$ and vector G represents additional terms in (9) and (10) which are dependent on $\dot{\gamma}$ and $\dot{\mu}$. We define $u_1 = \dot{\gamma}$ and $u_2 = \dot{\mu}$ and obtain (12) at the bottom of the page. By solving (11) for \dot{V} and $\dot{\psi}$, we obtain the set of nonlinear equations

$$\begin{bmatrix} \dot{V} \\ \dot{\psi} \end{bmatrix} = \begin{bmatrix} \bar{f}_1(x) \\ \bar{f}_2(x) \end{bmatrix} + \begin{bmatrix} \bar{g}_1(x) & \bar{g}_2(x) \\ \bar{g}_3(x) & \bar{g}_4(x) \end{bmatrix} \begin{bmatrix} u_1 \\ u_2 \end{bmatrix} \quad (13)$$

where

$$\begin{aligned} \begin{bmatrix} \bar{f}_1(x) \\ \bar{f}_2(x) \end{bmatrix} &= - \begin{bmatrix} A & B \\ D & E \end{bmatrix}^{-1} \begin{bmatrix} C \\ F \end{bmatrix} \omega \\ \begin{bmatrix} \bar{g}_1(x) & \bar{g}_2(x) \\ \bar{g}_3(x) & \bar{g}_4(x) \end{bmatrix} &= - \begin{bmatrix} A & B \\ D & E \end{bmatrix}^{-1} \bar{G}. \end{aligned}$$

$\bar{G}_{2N \times 2}$ is introduced as (A6) in Appendix A and satisfies $G = \bar{G}[u_1 \ u_2]^T$, and $\bar{f}_1, \bar{f}_2, \bar{g}_1, \bar{g}_2, \bar{g}_3, \bar{g}_4 \in R^N$.

Equation (13) is an affine nonlinear system in continuous-time with control inputs u_1 and u_2 . Once the control inputs are defined, the UPFC control parameters γ and μ can be obtained by integrating the control inputs. By Incorporating (1) and (2), we obtain the system dynamic equations as (14) at the bottom of the next page. Equation (14) is now in special case of strict feedback form [as explained after (18)] where backstepping can be used for the controller design.

Remark 1: In the case of multiple UPFCs in the network, (7)–(12) are repeated for each pair of UPFC buses t_j+n and

$$\begin{cases} G_t = +B_{t+n,h+n}V_{h+n}[u_1 \sin(\psi_{t+n} - \psi_{h+n}) + u_2 \cos(\psi_{t+n} - \psi_{h+n})] \\ G_h = -B_{t+n,h+n}V_{h+n}[u_1 \sin(\psi_{t+n} - \psi_{h+n}) + u_2 \cos(\psi_{t+n} - \psi_{h+n})] \\ G_{t+N} = -B_{t+n,h+n}V_{t+n}u_1 \\ G_{h+N} = +B_{t+n,h+n}V_{h+n}[u_1 \cos(\psi_{t+n} - \psi_{h+n}) - u_2 \sin(\psi_{t+n} - \psi_{h+n})] \\ G_i = 0, \quad \text{elsewhere} \end{cases} \quad (12)$$

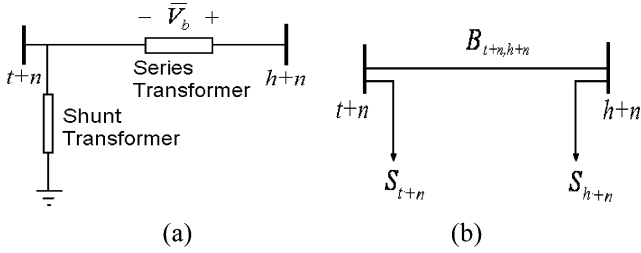


Fig. 1. (a) UPFC connected between two network nodes. (b) Injected powers to the connected buses.

$h_j + n$ for all $1 \leq j \leq k$, where k is the total number of UPFCs. Similarly, the corresponding entries of matrices A , B , D , and E change following the same logic described for (11). Moreover, vector G has entries corresponding to each UPFC. Consequently, the resulting differential equation is affine in terms of all UPFC control inputs which is given by

$$\begin{bmatrix} \dot{V} \\ \dot{\psi} \end{bmatrix} = \begin{bmatrix} \bar{f}_{T1}(x_T) \\ \bar{f}_{T2}(x_T) \end{bmatrix} + \sum_{j=1}^k \begin{bmatrix} \bar{g}_{j1}(x_T) & \bar{g}_{j2}(x_T) \\ \bar{g}_{j3}(x_T) & \bar{g}_{j4}(x_T) \end{bmatrix} \begin{bmatrix} u_{j1} \\ u_{j2} \end{bmatrix} \quad (15)$$

where k is the number of UPFCs and $x_T = [x_S^T \ \gamma_1 \ \mu_1 \ \cdots \ \gamma_k \ \mu_k]^T$. The nonlinear functions $\bar{f}_{T1}, \bar{f}_{T2}, \bar{g}_{j1}, \bar{g}_{j2}, \bar{g}_{j3}, \bar{g}_{j4} \in R^N$ are defined in Appendix A.

V. CONTROLLER DESIGN

The conventional approach to damping oscillations in an interconnected power system is to employ a linear control scheme [19]. By contrast, we target the stability of the generators in a nonlinear sense by defining an appropriate Lyapunov function. In the control development, we restrict our design to the case of constant loads. Also, we assume that the mechanical power P_{mi} ($1 \leq i \leq n-1$) is slowly changing compared to the other control variables; thus, $\dot{P}_{mi} \approx 0$. For the purpose of convenience we define new state variables as

$$\begin{aligned} x_{1i} &= \delta_i - \delta_{i0} \\ x_{2i} &= \omega_i \\ x_{3i} &= V_{i+n} \sin(\delta_i - \psi_{i+n}) \end{aligned} \quad (16)$$

where δ_{i0} is the pre-fault generator angle for $1 \leq i \leq n-1$. The selection of x_{3i} renders (2) in the backstepping form as will be explained. Using (15), we obtain

$$\begin{aligned} \dot{x}_{3i} &= \dot{V}_{i+n} \sin(\delta_i - \psi_{i+n}) \\ &\quad + V_{i+n}(\omega_i - \dot{\psi}_{i+n}) \cos(\delta_i - \psi_{i+n}) \\ &= \bar{f}_{T1i} \sin(\delta_i - \psi_{i+n}) - V_{i+n} \bar{f}_{T2i} \cos(\delta_i - \psi_{i+n}) \\ &\quad + V_{i+n} \omega_i \cos(\delta_i - \psi_{i+n}) \\ &\quad + \sum_{j=1}^k \{ [\bar{g}_{j1i} \sin(\delta_i - \psi_{i+n}) \\ &\quad - V_{i+n} \bar{g}_{j3i} \cos(\delta_i - \psi_{i+n})] u_{j1} \\ &\quad + [\bar{g}_{j2i} \sin(\delta_i - \psi_{i+n}) \\ &\quad - V_{i+n} \bar{g}_{j4i} \cos(\delta_i - \psi_{i+n})] u_{j2} \} \\ &= \bar{f}_{T1i}(x_T) + \sum_{j=1}^k a_{j1i}(x_T) u_{j1} + a_{j2i}(x_T) u_{j2} \end{aligned} \quad (17)$$

where $\bar{f}_{T1i}, \bar{f}_{T2i}, \bar{g}_{j1i}, \bar{g}_{j2i}, \bar{g}_{j3i}$, and \bar{g}_{j4i} are the i th elements of $\bar{f}_{T1}, \bar{f}_{T2}, \bar{g}_{j1}, \bar{g}_{j2}, \bar{g}_{j3}$, and \bar{g}_{j4} , respectively. Also, k is the number of UPFCs and j is the UPFC number.

A. Single Generator/Single UPFC Control

To introduce the design concept, we initially design a controller for a single generator/single UPFC power system using the standard backstepping design method with the control inputs $u_{j1} = u_1$ and $u_{j2} = u_2$. This approach will be extended to multiple generators/multiple UPFCs in the next section.

Remark 2: In [15], [18], and [22], it is demonstrated that if the UPFC injects the maximum series voltage (i.e., constant V_b), it can inject the maximum active power; thus, it improves transient stability. The condition $V_b = \text{Const}$ may be applied by noting that $\gamma^2 + \mu^2 = V_b^2$. This in turn results in $\gamma u_1 + \mu u_2 = 0$ by taking derivative from both sides (note that $dV_b^2/dt = 0$ for constant V_b) which may be considered as an algebraic relationship between the control inputs u_1 and u_2 . However, for damping the after-fault oscillations V_b can be kept high at the beginning (for a short time) and reduced afterwards in accordance with the state errors as this helps reduce the electrical stress on the UPFC. According to [18], UPFC injected power can also be controlled by varying V_b under the constant phase angle θ . Then, when θ is around $\pm 90^\circ$ maximum active power is injected for a given V_b . This requires that $\gamma = 0$, and thus, $u_1 = 0$.

$$\begin{cases} \dot{\delta}_i = \omega_i \\ M_i \dot{\omega}_i = P_{mi} - \frac{M_i}{M_T} P_{\text{COI}} - B_{i,i+n} E_{gi} V_{i+n} \sin(\delta_i - \psi_{i+n}); \quad i = 1, \dots, n \\ \begin{bmatrix} \dot{V} \\ \dot{\psi} \end{bmatrix} = \begin{bmatrix} \bar{f}_1(x) \\ \bar{f}_2(x) \end{bmatrix} + \begin{bmatrix} \bar{g}_1(x) & \bar{g}_2(x) \\ \bar{g}_3(x) & \bar{g}_4(x) \end{bmatrix} \begin{bmatrix} u_1 \\ u_2 \end{bmatrix} \\ \dot{\gamma} = u_1 \\ \dot{\mu} = u_2 \end{cases} \quad (14)$$

Consequently, in this design we let $u_1 = 0$ thereby decreasing the number of inputs in (17). Then, from (2), (16), and (17), the new set of state equations can be constructed as

$$\begin{cases} \dot{x}_{1i} = x_{2i} \\ M_i \dot{x}_{2i} = f_{1i} + g_{1i} x_{3i} \\ \dot{x}_{3i} = f_{2i}(x) + g_{2i}(x)u; i = 1, \dots, n \end{cases} \quad (18)$$

where $f_{1i} = P_{mi} - (M_i/M_T)P_{COI}$, $g_{1i} = -B_{i,i+n}E_{gi}$, $f_{2i}(x) = f_{Ti}(x)$, $g_{2i}(x) = a_{2i}(x)$, $a_{2i}(x) = a_{12i}(x)$ from (17), and $u = u_2$ for $1 \leq i \leq n-1$ where $x = [x_S^T, \gamma, \mu]^T$. Equation (18) is a special case of strict feedback form where f_{1i} and g_{1i} are constants instead of functions of the states.

Assumption 1: The control gain $g_{2i}(x)$ is bounded away from zero. Without loss of generality it will be assumed that $g_{2i}(x) > 0$.

This claim is supported by the fact that due to its continuity if $g_{2i}(x)$ changes sign, then it must pass through the origin. As a consequence, (18) encounters a singularity tending to make $[\gamma \ \mu]^T$ infinitely large. By selecting a proper place for the UPFC and setting appropriate design gains, we can avoid large control inputs.

Step 1: Introducing $K_{\delta i}$ and K_{Z1i} as design constants, we introduce $z_{1i} = x_{2i} + K_{\delta i}x_{1i}$ which results in

$$\dot{x}_{1i} = -K_{\delta i}x_{1i} + z_{1i}. \quad (19)$$

Consequently, by defining $z_{2i} = (x_{3i} - x_{3si})$ we have

$$M_i \dot{z}_{1i} = f_{1i} + M_i K_{\delta i} x_{2i} + g_{1i} x_{3si} + g_{1i} z_{2i} \quad (20)$$

where

$$x_{3si} = \frac{1}{g_{1i}} \times [-x_{1i} - f_{1i} - M_i K_{\delta i} x_{2i} - K_{Z1i} z_{1i}] \quad (21)$$

is chosen such that the Lyapunov function $L_{1i} = (1/2)x_{1i}^2 + (1/2)M_i z_{1i}^2$ has a negative definite derivative when $z_{2i} = 0$.

Step 2: Define the new Lyapunov function

$$L_{2i} = K_{atteni} \left(\frac{1}{2} x_{1i}^2 + \frac{1}{2} M_i z_{1i}^2 \right) + \frac{1}{2} z_{2i}^2 \quad (22)$$

with K_{atteni} being a design constant, we can easily show that $\dot{L}_{2i} = K_{atteni}(\dot{x}_{1i}x_{1i} + M_i \dot{z}_{1i}z_{1i}) + \dot{z}_{2i}z_{2i} < 0$ guaranteeing that the states x_{1i} , z_{1i} , and z_{2i} asymptotically converge to zero provided that $\dot{z}_{2i} = \nu_i$ where

$$\nu_i = -K_{atteni}z_{1i}g_{1i} - K_{Z2i}z_{2i} \quad (23)$$

and from (18)

$$\dot{z}_{2i} = f_{2i}(x) + g_{2i}(x)u - \dot{x}_{3si} \quad (24)$$

where

$$\dot{x}_{3si} = \frac{1}{g_{1i}} \times \left[-x_{2i} - K_{Z1i}K_{\delta i}x_{2i} - \frac{K_{\delta i}M_i + K_{Z1i}}{M_i}(f_{1i} + g_{1i}x_{3i}) \right]. \quad (25)$$

Equation (24) along with $\dot{z}_{2i} = \nu_i$ and (23) provides a solution for control input u in terms of nonlinear functions of states as

$$u = g_{2i}(x)^{-1}(\nu_i - f_{2i}(x) + \dot{x}_{3si}). \quad (26)$$

Remark 3: If the assumption made in Remark 2 is not applied (i.e., $u_1 \neq 0$), (26) will revert to

$$a_{1i}(x)u_1 + a_{2i}(x)u_2 = \nu_i - f_{2i}(x) + \dot{x}_{3si} \quad (27)$$

where $a_{1i}(x) = a_{11i}(x)$ from (17), which gives a linear relationship in terms of the control inputs. Then, a second relationship such as $\gamma u_1 + \mu u_2 = 0$ (mentioned in Remark 2) between u_1 and u_2 is needed to select them. Since optimal performance of UPFC is obtained by varying both the injected voltage V_b and angle θ , a second relationship between u_1 and u_2 can play an important role in achieving the controller.

B. Multiple Generator/Multiple UPFC Control

For the case of multiple generator control, the (24) is replaced by

$$\dot{z}_2 = f_3(x) + g_2(x)\bar{H}u \quad (28)$$

where $f_3(x) = f_2(x) - \dot{x}_{3s}$, $f_2 = [f_{21} \ \dots \ f_{2,n-1}]^T$, $g_2 = \text{diag}(g_{21} \ \dots \ g_{2,n-1})$, $x_{3s} = [x_{3s1} \ \dots \ x_{3s,n-1}]^T$, and $\bar{H}_{(n-1) \times 1} = [1 \ \dots \ 1]^T$. Also, define $x_1 = [x_{11} \ \dots \ x_{1,n-1}]^T$, $z_1 = [z_{11} \ \dots \ z_{1,n-1}]^T$, and $z_2 = [z_{21} \ \dots \ z_{2,n-1}]^T$. Note that for the multiple UPFC case x is replaced by x_T and the dimensions of g_2 change. Moreover, note that only $n-1$ generators are chosen to be controlled. Since the n generators are present in the interconnected power network, the n th generator is forced to be controlled by the power balance if the remaining $n-1$ speeds are controlled. Since there are fewer inputs than outputs, it is generally difficult to find an input that makes the first derivative of the Lyapunov function candidate negative definite. In other words, because of the inconsistency that arises due to multiple solutions for a single u the above single generator control method cannot be employed for multiple generator control. Thus, we propose the input

$$u = \frac{-1}{\sum_{i=1}^{n-1} (1 + 2K_{Z3}z_{2i})g_{2i}} \times \left((\bar{H}^T + 2K_{Z3}z_2^T) f_3(x) + (\bar{H}^T + K_{Z3}z_2^T) K_{Z2}z_2 \right) \quad (29)$$

where K_{Z2} and K_{Z3} are design parameters.

Definition [Uniformly Ultimately Bounded (UUB)] [20]: Consider the dynamical system $\dot{x} = f(x)$ with $x \in \mathbb{R}^n$ being a state vector. Let the initial time be t_0 and initial condition be $x_0 = x(t_0)$. Then, the equilibrium point x_e is said to be UUB if there exists a compact set $S \subset \mathbb{R}^n$ so that for all $x_0 \in S$ there exists a bound B and a time $T(B, x_0)$ such that $\|x(t) - x_e\| \leq B$ for $\forall t > t_0 + T$.

Theorem 1: Consider the dynamical system described by (19), (20), and (24) which is rewritten as

$$\begin{cases} \dot{x}_{1i} = -K_{\delta i} x_{1i} + z_{1i} \\ M_i \dot{z}_{1i} = f_{1i} + M_i K_{\delta i} x_{2i} + g_{1i} x_{3i} + g_{1i} z_{2i} \\ \dot{z}_{2i} = f_{2i}(x) + g_{2i}(x)u - \dot{x}_{3i} \end{cases} \quad (30)$$

with the input given by (29) for $1 \leq i \leq n-1$. Then the states are globally uniformly ultimately bounded provided Assumption 1 holds.

Proof: See Appendix B. ■

Remark 4: Equation (30) needs the term $\sum_{i=1}^{n-1} (1 + 2K_{Z3} z_{2i}^T) g_{2i}$ to be bounded away from zero. Based on Assumption 1, this can be easily achieved by selecting a proper K_{Z2} and K_{Z3} and replacing each x_{3i} with $K_{MZ2i} x_{3i}$ where K_{MZ2i} is a proper modification factor if $\sum_{i=1}^{n-1} (1 + 2K_{Z3} z_{2i}^T) g_{2i} = 0$. From (18) this changes g_{2i} to $K_{MZ2i} g_{2i}$ such that the term $\sum_{i=1}^{n-1} (1 + 2K_{Z3} z_{2i}^T) K_{MZ2i} g_{2i}$ moves from zero in (29).

VI. NEURAL NETWORK CONTROL

Although (29) provides the UPFC control inputs, finding the analytical and/or numerical nonlinear control inputs in practice (for fast computing) is a challenging task in large power systems. Moreover, in order to implement the control law, a complete knowledge of the total power system dynamics and topology are needed. However, by using the neural network approximation property for nonlinear functions with online learning scheme [20], we are able to approximate the nonlinear ‘‘unknown dynamic’’ terms in the power system dynamics, thus relaxing the need for a complete system description as well as onerous function calculations.

A general function $f(x) \in R$ where $x \in R^n$ can be written as $f(x) = W^T \phi(\bar{V}^T x) + \varepsilon(x)$ with $\varepsilon(x)$ a neural network (NN) functional reconstruction error where $W \in R^{N_2 \times 1}$ and $\bar{V} \in R^{n \times N_2}$ are weight matrices [20]. In our design, input-to-the-hidden-layer weight matrix \bar{V} is selected initially at random and held fixed during learning. It is demonstrated in [21] that if the input-to-the-hidden-layer weights, \bar{V} , are chosen initialized randomly and kept constant and if the number of neurons N_2 in the hidden layer is sufficiently large, the NN approximation error $\varepsilon(x)$ can be made arbitrarily small since the activation function vector ϕ forms a basis.

A. Single Generator/Single UPFC Control

Consider the system (18). Unlike (26), here we assume that the nonlinear functions g_{2i} and f_{2i} (for $1 \leq i \leq n-1$) are not available. Thus, in order to provide the desired input we employ the neural network approximation property for nonlinear functions as $u_1 = -K_{Z2i} z_{2i} - (W_i^T \phi_i(\bar{V}_i^T x) + \varepsilon)$ where the term $W_i^T \phi_i(\bar{V}_i^T x) + \varepsilon$ represents the unknown nonlinear

function in the control input with W_i being unknown ideal weight matrix (where $\|W_i\|$ is assumed to be upper bounded [20]) and $|\varepsilon_i| \leq \varepsilon_M$ is the approximation error in a compact set $\Omega = \{x_{1i}, z_{1i}, z_{2i} \mid x_{1i}^2 + z_{1i}^2 + z_{2i}^2 \leq \rho\}$. In practice, the actual weight matrix W_i and approximation error ε_i are unknown and only an estimation of the weight matrix is utilizable, i.e.,

$$u = -K_{Z2i} z_{2i} - \hat{W}_i^T \phi_i(\bar{V}_i^T x). \quad (31)$$

It is shown in Appendix C that the states $[z_{2i} \quad \hat{W}_i^T]^T$ are stable with arbitrarily small upper bounds by selecting the neural network weight update law as [20]

$$\dot{\hat{W}}_i = \Gamma_i \phi_i(\bar{V}_i^T x) z_{2i} - \alpha_i \Gamma_i \hat{W}_i \quad (32)$$

where α_i is a design constant and Γ_i is a design constant matrix.

B. Multiple Generator/Multiple UPFC Control

By using the similar approach to single generator neural network controller we define the desired control input for system (18) as (33)

$$u = -K_{Z2} \bar{H}^T z_2 - (W^T \varphi(\bar{V}^T x) + \varepsilon) \quad (33)$$

where $|\varepsilon| \leq \varepsilon_M$ in a compact set [20] $\Omega = \{x_1, z_1, z_2 \mid x_1^T x_1 + z_1^T z_1 + z_2^T z_2 \leq \rho\}$. Then we utilize the estimation of the weight matrix to obtain

$$u = -K_{Z2} \bar{H}^T z_2 - \hat{W}^T \varphi(\bar{V}^T x). \quad (34)$$

It is shown in Appendix D that by selecting the weight update law as

$$\dot{\hat{W}} = \Gamma \phi(\bar{V}^T x) \bar{H}^T z_2 - \alpha \Gamma \hat{W} \quad (35)$$

boundedness of the states $[\bar{H}^T z_2 \quad \|\hat{W}\|]^T$ with bounds defined in the Appendix is achieved. In general, it is hard to conclude stability of the states z_{2i} ($1 \leq i \leq n-1$) from boundedness of $\bar{H}^T z_2$. However, in this problem we have considered $n-1$ generator to avoid dependency of generators electrical powers (and z_{2i}) to each other. For many power system topologies if the UPFC is placed on the proper bus we may conclude stability of z_{2i} ($1 \leq i \leq n-1$) based on the stability of $\bar{H}^T z_2$ as confirmed by simulations. Exceptions may include topologies with isolated generators. Similar to proof of Theorem 1, this yields stability of the states x_1 and z_1 .

Remark 5: We can see from (34) and (35) that the control and update laws are only functions of generators data and loads. Although for the controller design δ_{i0} is needed, this parameter can be achieved by knowing the generator operating conditions. Thus, no prior knowledge of power system topology is needed for controller design.

VII. SIMULATION RESULTS

For control validation, two power system topologies are considered. In both examples the simulations are performed using

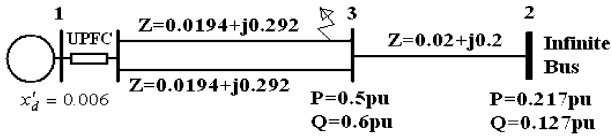


Fig. 2. One-generator power system.

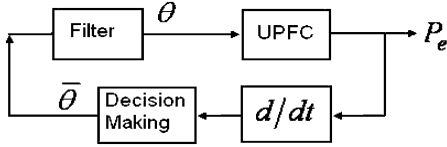
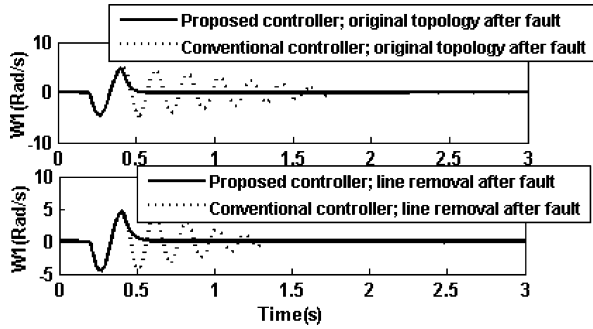


Fig. 3. UPFC active power controller.

Fig. 4. Damping effect of the proposed nonlinear controller when compared to the method with UPFC fixed injected voltage V_b and variable angle θ .

the complete power system model (with line resistances) to evaluate the effectiveness of the modeling and design. Also, steam governor is in action in all simulations. First, the system in Fig. 2 is chosen where a three-phase fault is injected close to bus 3 (as depicted in Fig. 2) at $t = 0.2$ s and removed at $t = 0.4$ s. The infinite bus is simulated by a huge generator whose angle and speed do not change by the fault. The infinite bus voltage and angle are given as $V_2 = 1.0470$ pu and $\psi_2 = -0.0091$ Rad. The data for generator 1 are given as $x'_d = 0.006$, $H = 1$, $E_g = 1.0657$ pu, and $\delta = 0.0017$ Rad at $t = 0$. The UPFC is placed on bus 1 between buses 1 and 3 and is activated after fault clearance.

Two scenarios are assumed; the fault is removed without changing the topology and with removal of one of the lines between buses 1 and 3 (i.e., the faulted line.) In accordance with Remark 2, the proposed control is performed via constant UPFC angle $\theta = \pm 90^\circ$ and variable (controlled) UPFC voltage V_b . The design is performed by using the method introduced in Section V-A for single generator control where gains are chosen as $K_{\delta 1} = 0.1$, $K_{Z11} = 0.2$, $K_{Z12} = 100$, and $K_{atten} = 1$. The results from the proposed method are compared with the case with $V_{b\max} = 0.5$ pu and variable θ where the controller examines the slope of the power flow in the line, where the UPFC series transformer is placed, and switches the output $\bar{\theta}$ (shown in Fig. 3) between $\pm 90^\circ$ (which gives maximum UPFC injected power at constant $V_b = V_{b\max}$ as explained in Remark 2) correspondingly to prevent increasing or decreasing the flow of power in the UPFC line, and thus, to prevent the power flow oscillations. The output $\bar{\theta}$ is then passed through a first order filter $K_P/(1 + \tau_P s)$ (with $K_P = 0.1$; $\tau_P = 0.1$ after fine

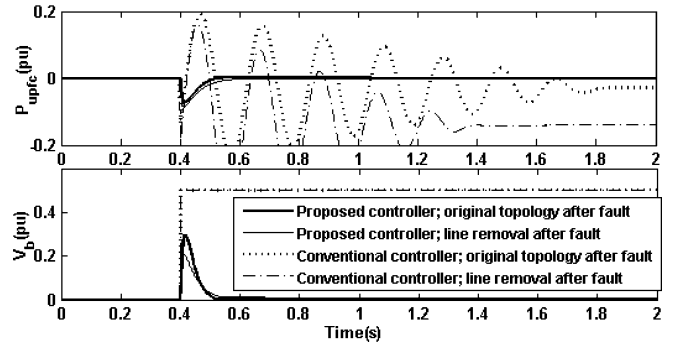
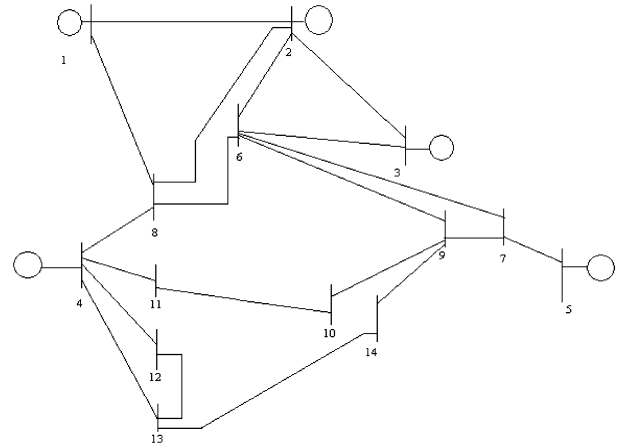
Fig. 5. UPFC injected power and voltage in the proposed controller when compared to the method with UPFC fixed voltage V_b and variable angle θ .

Fig. 6. The IEEE 14-bus, five-generator power system.

TABLE I
GENERATORS SPECIFICATIONS

Gen no.	1	2	3	4	5
x'_d	0.006	0.006	0.006	0.006	0.006
$H = \omega_s M/2$	5	1	1	5	5

tuning), depicted in Fig. 3, to reduce sharp power fluctuations and to provide the UPFC angle θ which in turn provides the total line power P_e (including the injected power by UPFC).

Figs. 4 and 5 show the UPFC damping effect, injected power, and voltage of the proposed controller for the two scenarios (original topology and line removal after fault) as compared to those of the conventional controller through controlling θ . As shown in the figures faster damping as well as lower voltage and injected power are achieved by using the proposed nonlinear controller. Also, unlike the conventional controller, no significant difference in controller performance between the two cases (original topology and line removal after fault) is observed when using the proposed controller.

In the second example the IEEE 14-bus, five-generator power system shown in Fig. 6 is used and subjected to three phase faults.

The generator data are given in Table I. All the generators have steam governors and the UPFC control is implemented to stabilize the power system. The power system loads are considered as constants. The control objective is to damp the generators oscillations after the fault is cleared.

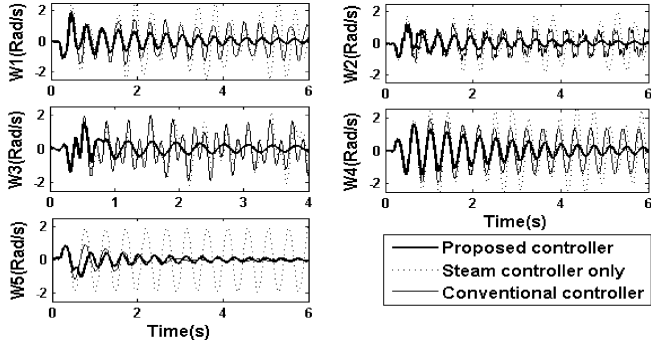


Fig. 7. Generator speeds with and without control; Case 1 with fault on bus 1.

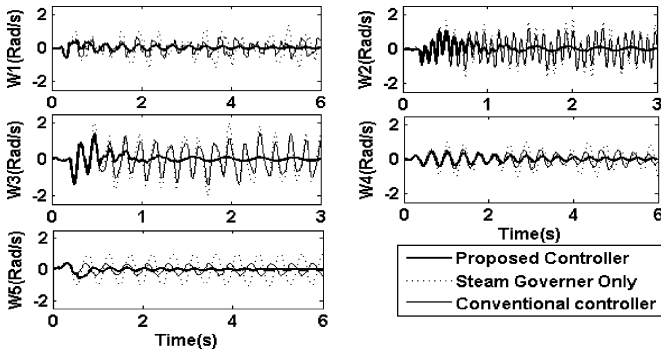


Fig. 8. Generator speeds with and without control; Case 1 with fault on bus 6.

In the system given by Fig. 6, the UPFC is installed on bus 6 between buses 6 and 7 which is found to be an appropriate placement by trial and error, i.e., it can stabilize the power system for different fault locations. The power system modes are 11.3561, 5.9101, 2.6977, and 2.1026 Hz. A three-phase short circuit fault is applied to buses 1, 6, and 11 at $t = 0.2$ s and removed at $t = 0.4$ s. Generators 1 through 4 are chosen for control. The control inputs γ and μ are initially set to zero such that $V_b(t_0) = 0$ and the proposed control method is performed through using variable V_b and $\theta = \pm 90^\circ$. Two cases are considered for simulations.

Case 1: All power system dynamic states are assumed to be available for the control design and (29) along with $\theta = \pm 90^\circ$ ($u_1 = 0$) are used to design the controller. The design gains are chosen as $K_{\delta 1}$ through $K_{\delta 4} = 0.1$, K_{Z11} through $K_{Z14} = 0.2$, $K_{Z2} = 100$, $K_{Z3} = 1$.

Figs. 7–9 show that significant percentage of oscillation damping can be achieved for a medium size power network by using a single UPFC as a controller. Moreover, the nonlinear controller without changing the controller gains from the previous case is able to damp the oscillations resulting from a fault occurring at different locations through satisfactory control effort as shown in Figs. 10 and 11. Note, however, that damping performance varies with the fault location. In particular, Figs. 7–9 illustrate that for faults occurring at the locations relatively close to the UPFC bus (bus 6), the oscillation damping is more effective than for the faults occurring far from UPFC bus. Also, the control effort for the latter case is higher as shown in Figs. 10 and 11. This is due to different after fault conditions imposed on the controller.

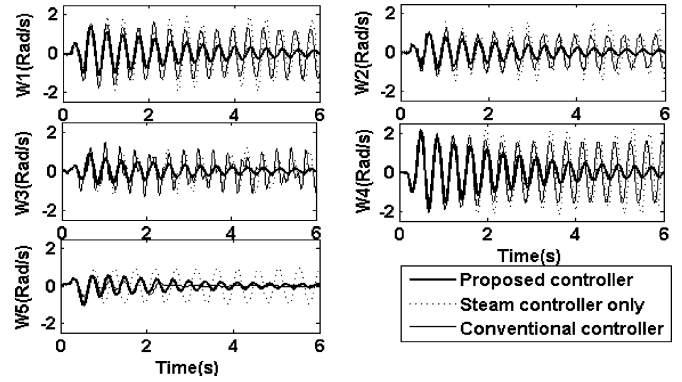


Fig. 9. Generator speeds with and without control; Case 1 with fault on bus 11.

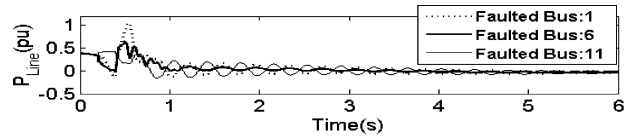


Fig. 10. Active power flow from bus 6 to 7; Case 1.

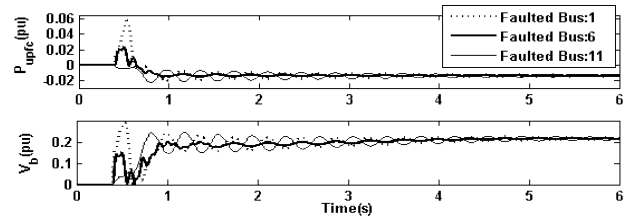


Fig. 11. UPFC injected power and series voltage; Case 1.

However, the voltage and line flows do not go back to their pre-fault values due to bounded stability performance of the controller. Overall, from these results, the proposed control is very effective in damping the oscillations even in the presence of numerous modes and with significant fault (as illustrated in Figs. 4–9) occurring in the power network. The results from the proposed controller are then compared with those of the conventional controller explained in the first example with $K_P = 0.2$; $\tau_P = 0.1$ (after fine tuning) where instead of observing the line power flow slope, the sign change in angle difference of the UPFC line buses (i.e., $\text{sign}(\psi_{t+n} - \psi_{h+n})$) is considered since a stabilizing controller using the power flow derivative sign was not achieved. Unlike the previous example, the conventional controller cannot stabilize all generators and only affects the generator close to UPFC (i.e., Gen5). For the fault on bus 6, no significant damping effect is introduced by the conventional controller.

Case 2: Power system dynamics are assumed unavailable. By using (34) and (35) and assuming $u_1 = 0$ ($\theta = \pm 90^\circ$), the NN controller is utilized to approximate the unknown system. Ten neurons are selected for the hidden layer with sigmoid [20] as activation function and design gains are chosen as $K_{\delta 1} = 0.1$, $K_{\delta 2} = 0.2$, $K_{\delta 3} = 0.1$, $K_{\delta 4} = 0.1$, K_{Z11} through $K_{Z14} = 0.1$, $K_{Z2} = 500$, $\alpha = 1e - 4$, and $\Gamma = 5e5$. The weight estimate \hat{W} is initialized randomly. No offline training is utilized to tune the weights and no *a priori* data about the power system topology is needed for controller design.

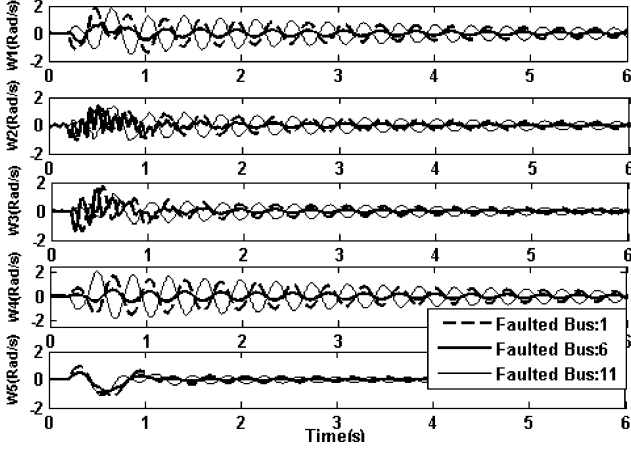


Fig. 12. Generator speeds; Case 2.

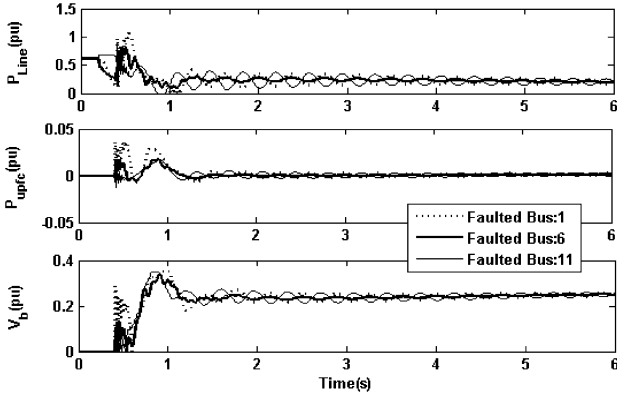


Fig. 13. UPFC injected power and series voltage; Case 2.

Figs. 12 and 13 illustrate that the neural network controller nearly has the same ability to damp the oscillations as the controller in Case 1. This implies that the neural network controller is able to quickly learn the power system nonlinear dynamics by only using the network voltages, angles, and speeds as well as the synthesized input u .

VIII. CONCLUSION

We have introduced a general nonlinear dynamical model for power systems with UPFC as stabilizing controller. This model is free of algebraic equations, thus conventional nonlinear control strategies are applicable to stabilize the power system after fault occurrence. We have addressed a multi-machine control scheme in which the number of control inputs is less than the number of outputs. Furthermore, we have utilized neural networks approximation property to relax the burdensome nonlinear function calculations and *a priori* knowledge about the power system dynamics needed for control design. Our analytical approach as well as our simulation results shows the effectiveness of our approach.

APPENDIX A

According to (4) and (5) we have

$$\begin{aligned} \dot{S}_P = & \dot{P}_{Li} + \dot{V}_i \left(\sum_{j=1}^n B_{ij} E_{gj} \sin(\psi_i - \delta_j) \right. \\ & \left. + \sum_{j=n+1}^{n+N} B_{ij} V_j \sin(\psi_i - \psi_j) \right) \\ & + \dot{\psi}_i V_i \sum_{j=1}^n B_{ij} E_{gj} \cos(\psi_i - \delta_j) \\ & - V_i \sum_{j=1}^n B_{ij} E_{gj} \omega_j \cos(\psi_i - \delta_j) \\ & + V_i \sum_{j=n+1}^{n+N} B_{ij} \sin(\psi_i - \psi_j) \dot{V}_j \\ & + \dot{\psi}_i V_i \sum_{j=n+1}^{n+N} B_{ij} V_j \cos(\psi_i - \delta_j) \\ & - V_i \sum_{j=n+1}^{n+N} B_{ij} V_j \cos(\psi_i - \psi_j) \dot{\psi}_j = 0 \quad (A1) \end{aligned}$$

$$\begin{aligned} \dot{S}_Q = & -\dot{Q}_{Li} + \dot{V}_i \left(\sum_{j=1}^n B_{ij} E_{gj} \cos(\psi_i - \delta_j) \right. \\ & \left. + \sum_{j=n+1}^{n+N} B_{ij} V_j \cos(\psi_i - \psi_j) \right) \\ & - \dot{\psi}_i V_i \sum_{j=1}^n B_{ij} E_{gj} \sin(\psi_i - \delta_j) \\ & + V_i \sum_{j=1}^n B_{ij} E_{gj} \omega_j \sin(\psi_i - \delta_j) \\ & + V_i \sum_{j=n+1}^{n+N} B_{ij} V_j \sin(\psi_i - \psi_j) \dot{\psi}_j = 0. \quad (A2) \end{aligned}$$

Entries of matrices $\bar{A}_{N \times N}$, $\bar{B}_{N \times N}$, $C_{N \times n}$, $\bar{D}_{N \times N}$, $\bar{E}_{N \times N}$, and $F_{N \times n}$ for the case without UPFC are summarized as follows:

$$a_{ij} = B_{i+n, j+n} V_{i+n} \sin(\psi_{i+n} - \psi_{j+n}) \quad i = 1, \dots, N; j = 1, \dots, N; i \neq j \quad (A3a)$$

$$\begin{aligned} a_{ii} = & \sum_{j=1}^n B_{i+n, j} E_{gj} \sin(\psi_{i+n} - \delta_j) \\ & + \sum_{j=1}^N B_{i+n, j+n} V_{j+n} \sin(\psi_{i+n} - \psi_{j+n}) \\ & + \frac{\partial P_{Li+n}}{\partial V_{i+n}} \quad i = 1, \dots, N \quad (A3b) \end{aligned}$$

$$b_{ij} = -V_{i+n} B_{i+n, j+n} V_{j+n} \cos(\psi_{i+n} - \psi_{j+n}) \quad i = 1, \dots, N; j = 1, \dots, N; i \neq j \quad (A3c)$$

$$\begin{aligned}
b_{ii} = & V_{i+n} \sum_{j=1}^n B_{i+n,j} E_{gj} \cos(\psi_{i+n} - \delta_j) \\
& + V_{i+n} \sum_{j=n+1}^{n+N} B_{i+n,j} V_j \cos(\psi_{i+n} - \psi_j) \\
& - V_{i+n}^2 B_{i+n,i+n} + \frac{\partial P_{Li+n}}{\partial \psi_{i+n}} \quad i = 1, \dots, N
\end{aligned} \tag{A3d}$$

$$\begin{aligned}
c_{ij} = & -V_{i+n} B_{i+n,j} E_{gj} \cos(\psi_{i+n} - \delta_j) \\
& \quad i = 1, \dots, N; j = 1, \dots, n
\end{aligned} \tag{A3e}$$

$$\begin{aligned}
d_{ij} = & B_{i+n,j+n} V_{i+n} \cos(\psi_{i+n} - \psi_{j+n}) \\
& \quad i = 1, \dots, N; j = 1, \dots, N; i \neq j
\end{aligned} \tag{A4a}$$

$$\begin{aligned}
d_{ii} = & \sum_{j=1}^n B_{i+n,j} E_{gj} \cos(\psi_{i+n} - \delta_j) \\
& + \sum_{j=1}^N B_{i+n,j+n} V_{j+n} \cos(\psi_{i+n} - \psi_{j+n}) \\
& + B_{i+n,i+n} V_{i+n} - \frac{\partial Q_{Li+n}}{\partial V_{i+n}}; \quad i = 1, \dots, N
\end{aligned} \tag{A4b}$$

$$\begin{aligned}
e_{ij} = & V_{i+n} B_{i+n,j+n} V_{j+n} \sin(\psi_{i+n} - \psi_{j+n}) \\
& \quad i = 1, \dots, N; j = 1, \dots, N; i \neq j
\end{aligned} \tag{A4c}$$

$$\begin{aligned}
e_{ii} = & -V_{i+n} \sum_{j=1}^n B_{i+n,j} E_{gj} \sin(\psi_{i+n} - \delta_j) \\
& - V_{i+n} \sum_{j=1}^N B_{i+n,j+n} V_{j+n} \sin(\psi_{i+n} - \psi_{j+n}) \\
& - \frac{\partial Q_{Li+n}}{\partial \psi_{i+n}} \quad i = 1, \dots, N
\end{aligned} \tag{A4d}$$

$$\begin{aligned}
f_{ij} = & V_{i+n} B_{i+n,j} E_{gj} \sin(\psi_{i+n} - \delta_j) \\
& \quad i = 1, \dots, N; j = 1, \dots, n.
\end{aligned} \tag{A4e}$$

Modifications on the entries of matrices $A_{N \times N}$, $B_{N \times N}$, $D_{N \times N}$, and $E_{N \times N}$ for the case with UPFC are summarized in (A5a)–(A5d) at the bottom of the page. The subscript (old) refers to the original values (without UPFC) as defined by (A3) and (A4).

The matrix \bar{G} is defined as follows:

$$\begin{cases} \bar{G}_{t,1} = +B_{t+n,h+n} V_{h+n} \sin(\psi_{t+n} - \psi_{h+n}) \\ \bar{G}_{t,2} = +B_{t+n,h+n} V_{h+n} \cos(\psi_{t+n} - \psi_{h+n}) \\ \bar{G}_{h,1} = -B_{t+n,h+n} V_{h+n} \sin(\psi_{t+n} - \psi_{h+n}) \\ \bar{G}_{h,2} = -B_{t+n,h+n} V_{h+n} \cos(\psi_{t+n} - \psi_{h+n}) \\ \bar{G}_{t+N,1} = -B_{t+n,h+n} V_{t+n} \\ \bar{G}_{t+N,2} = 0 \\ \bar{G}_{h+N,1} = +B_{t+n,h+n} V_{h+n} \cos(\psi_{t+n} - \psi_{h+n}) \\ \bar{G}_{h+N,2} = -B_{t+n,h+n} V_{h+n} \sin(\psi_{t+n} - \psi_{h+n}) \\ \bar{G}_{i,j} = 0; \quad \text{elsewhere.} \end{cases} \tag{A6}$$

For the case of multiple UPFCs matrices A , B , D , and E are changed to A_T , B_T , D_T , and E_T as described in Remark 1. The nonlinear functions used in (15) are described as

$$\begin{bmatrix} \bar{f}_{T1}(x_T) \\ \bar{f}_{T2}(x_T) \end{bmatrix} = - \begin{bmatrix} A_T(x_T) & B_T(x_T) \\ D_T(x_T) & E_T(x_T) \end{bmatrix}^{-1} \begin{bmatrix} C(x_T) \\ F(x_T) \end{bmatrix} \omega. \tag{A7}$$

Also, we have

$$\begin{aligned}
& - \begin{bmatrix} A_T(x_T) & B_T(x_T) \\ D_T(x_T) & E_T(x_T) \end{bmatrix}^{-1} G_T \\
& = - \begin{bmatrix} A_T(x_T) & B_T(x_T) \\ D_T(x_T) & E_T(x_T) \end{bmatrix}^{-1} \bar{G}_T U
\end{aligned} \tag{A8}$$

where

$U_{2k \times 1} = [u_{11} \ u_{21} \ \dots \ u_{1j} \ u_{2j} \ \dots \ u_{1k} \ u_{2k}]^T$, k is the number of UPFCs and $\bar{G}_T = [\bar{G}_{T1} \ \dots \ \bar{G}_{Tj} \ \dots \ \bar{G}_{Tk}]_{2N \times 2k}$ with $\bar{G}_{Tj} \in R^{2N \times 2}$ corresponds to the j th UPFC whose entries are defined in (A6). Using \bar{G}_T , we are able to define

$$\begin{aligned}
& \begin{bmatrix} \bar{g}_{j1}(x_T) & \bar{g}_{j2}(x_T) \\ \bar{g}_{j3}(x_T) & \bar{g}_{j4}(x_T) \end{bmatrix}_{2N \times 2} \\
& = - \begin{bmatrix} A_T(x_T) & B_T(x_T) \\ D_T(x_T) & E_T(x_T) \end{bmatrix}^{-1} \times G_{Tj}.
\end{aligned} \tag{A9}$$

$$\begin{cases} a_{t,h} = a_{t,h(\text{old})} + B_{t+n,h+n} [\gamma \sin(\psi_{t+n} - \psi_{h+n}) + \mu \cos(\psi_{t+n} - \psi_{h+n})] \\ b_{t,t} = b_{t,t(\text{old})} + B_{t+n,h+n} V_{h+n} [\gamma \cos(\psi_{t+n} - \psi_{h+n}) - \mu \sin(\psi_{t+n} - \psi_{h+n})] \\ b_{t,h} = b_{t,h(\text{old})} - B_{t+n,h+n} V_{h+n} [\gamma \cos(\psi_{t+n} - \psi_{h+n}) - \mu \sin(\psi_{t+n} - \psi_{h+n})] \end{cases} \tag{A5a}$$

$$\begin{cases} a_{h,h} = a_{h,h(\text{old})} - B_{t+n,h+n} [\gamma \sin(\psi_{t+n} - \psi_{h+n}) + \mu \cos(\psi_{t+n} - \psi_{h+n})] \\ b_{h,t} = b_{h,t(\text{old})} - B_{t+n,h+n} V_{h+n} [\gamma \cos(\psi_{t+n} - \psi_{h+n}) - \mu \sin(\psi_{t+n} - \psi_{h+n})] \\ b_{h,h} = b_{h,h(\text{old})} + B_{t+n,h+n} V_{h+n} [\gamma \cos(\psi_{t+n} - \psi_{h+n}) - \mu \sin(\psi_{t+n} - \psi_{h+n})] \end{cases} \tag{A5b}$$

$$d_{t,t} = d_{t,t(\text{old})} - B_{t+n,h+n} \gamma \tag{A5c}$$

$$\begin{cases} d_{h,h} = d_{h,h(\text{old})} + B_{t+n,h+n} [\gamma \cos(\psi_{t+n} - \psi_{h+n}) - \mu \sin(\psi_{t+n} - \psi_{h+n})] \\ e_{h,t} = e_{h,t(\text{old})} - B_{t+n,h+n} V_{h+n} [\gamma \sin(\psi_{t+n} - \psi_{h+n}) + \mu \cos(\psi_{t+n} - \psi_{h+n})] \\ e_{h,h} = e_{t,h(\text{old})} + B_{t+n,h+n} V_{h+n} [\gamma \sin(\psi_{t+n} - \psi_{h+n}) + \mu \cos(\psi_{t+n} - \psi_{h+n})] \end{cases} \tag{A5d}$$

APPENDIX B

Proof of Theorem 1: For the case of multiple generator control, we define the Lyapunov function as

$$L = \frac{1}{2} \left[\sum_{i=1}^{n-1} (z_{2i} + K_{Z3} z_{2i}^2) \right]^2 \quad (B1)$$

where K_{Z3i} is a design constant. Taking derivative of (B1), we have

$$\dot{L} = \left(\sum_{i=1}^{n-1} (1 + 2K_{Z3} z_{2i}) \dot{z}_{2i} \right) \left(\sum_{i=1}^{n-1} (z_{2i} + K_{Z3} z_{2i}^2) \right). \quad (B2)$$

Using the following equation:

$$\sum_{i=1}^{n-1} (1 + 2K_{Z3} z_{2i}) \dot{z}_{2i} = \sum_{i=1}^{n-1} \bar{v}_i \quad (B3)$$

where $\bar{v}_i = -K_{Z2}(z_{2i} + K_{Z3} z_{2i}^2)$, makes \dot{L} negative definite.

In order to obtain u_1 in the case of multiple generator control we use (24) and (B3) and obtain

$$u_1 = \left(\sum_{i=1}^{n-1} (1 + 2K_{Z3} z_{2i}) g_{2i}(x) \right)^{-1} \times \sum_{i=1}^{n-1} (\bar{v}_i - (1 + 2K_{Z3} z_{2i}) (f_{2i}(x) - \dot{x}_{3si})). \quad (B4)$$

The control input (B4) causes the term $\sum_{i=1}^{n-1} z_{2i} + K_{Z3} z_{2i}^2$ converge to zero asymptotically. Consequently, z_{2i} converges to the bound obtained as follows:

$$\sum_{i=1}^{n-1} z_{2i} + K_{Z3} z_{2i}^2 = \sum_{i=1}^{n-1} K_{Z3} \left(\left(z_{2i} + \frac{1}{2K_{Z3}} \right)^2 - \frac{1}{4K_{Z3}^2} \right) = 0$$

which in turns results in the bound

$$\sum_{i=1}^{n-1} \left(z_{2i} + \frac{1}{2K_{Z3}} \right)^2 = \frac{n-1}{4K_{Z3}^2}. \quad (B5)$$

Thus, z_{2i} approaches to the bound presented by (B5) asymptotically.

Next, (30) implies

$$\begin{bmatrix} \dot{x}_{1i} \\ \dot{z}_{1i} \end{bmatrix} = \begin{bmatrix} -K_{\delta i} & 1 \\ -\frac{1}{M_i} & -\frac{K_{Z1i}}{M_i} \end{bmatrix} \begin{bmatrix} x_{1i} \\ z_{1i} \end{bmatrix} + \begin{bmatrix} 0 \\ \frac{g_{1i}}{M_i} \end{bmatrix} z_{2i}; \quad 1 \leq i \leq n-1 \quad (B6)$$

which is a linear input-to-state stable system by proper choice of the control gains $K_{\delta i}$ and K_{Z1i} such that the eigenvalues of the linear system have negative real parts. Thus, the states x_{1i} and z_{1i} are bounded following the stability of z_{2i} for $1 \leq i \leq n-1$. ■

APPENDIX C

Equation (24) for the i th generator in a single-UPFC power system can be written as

$$\dot{z}_{2i} = g_{2i} \left(\frac{f_{2i}(x) - \dot{x}_{3si}}{g_{2i}(x)} + u \right) \quad (C1)$$

where x is the vector of the global parameters as defined earlier. We repeat the back stepping control design mentioned in the previous section and define the Lyapunov function L_{2i} as

$$L_{2i} = z_{2i}^2 / (2g_{2i}(x)) \quad (C2)$$

which has the derivative as

$$\dot{L}_{2i} = \left(\frac{\dot{z}_{2i}}{g_{2i}(x)} - \frac{\dot{g}_{2i}(x)}{2g_{2i}^2(x)} z_{2i} \right) z_{2i}. \quad (C3)$$

Applying (C1) to (C3) renders the Lyapunov function derivative $\dot{L}_{2i} < 0$ provided the control input is selected as

$$u = -K_{Z2i} z_{2i} - \frac{f_{2i}(x) - \dot{x}_{3si}}{g_{2i}(x)} + \frac{\dot{g}_{2i}(x)}{2g_{2i}^2(x)} z_{2i}. \quad (C4)$$

The term $(f_{2i}(x) - \dot{x}_{3si}) / (g_{2i}(x)) - (\dot{g}_{2i}(x)) / (2g_{2i}^2(x)) z_{2i}$ in (C4) is the unknown term which must be approximated by a neural network as

$$\frac{f_{2i}(x) - \dot{x}_{3si}}{g_{2i}(x)} - \frac{\dot{g}_{2i}(x)}{2g_{2i}^2(x)} z_{2i} = W_i^T \phi_i(\bar{V}_i^T x) + \varepsilon_i \quad (C5)$$

where $|\varepsilon_i| \leq \varepsilon_M$ is the approximation error in a compact set [20] $\Omega = \{x_{1i}, z_{1i}, z_{2i} | x_{1i}^2 + z_{1i}^2 + z_{2i}^2 \leq \rho\}$. Since the ideal weights W_i are not known, the estimated weight matrix \hat{W}_i is utilized to approximate u_1 as (31). Now, define the Lyapunov function

$$L_i = L_{2i} + (1/2) \tilde{W}_i^T \Gamma_i^{-1} \tilde{W}_i \quad (C6)$$

where $\tilde{W}_i = \hat{W}_i - W_i$ and Γ_i is a design constant matrix. Taking the derivative of (C6) and applying (31) results in

$$\dot{L}_i = -K_{Z2i} z_{2i}^2 - \tilde{W}_i^T \phi_i(\bar{V}_i^T x) z_{2i} + \varepsilon_i z_{2i} + \tilde{W}_i^T \Gamma_i^{-1} \dot{\tilde{W}}_i. \quad (C7)$$

By selecting the neural network weight update law as (32) and applying (C7) we obtain

$$\begin{aligned} \dot{L}_{2i} &= -K_{Z2i} z_{2i}^2 - \alpha_i \tilde{W}_i^T \dot{\tilde{W}}_i + \varepsilon_i z_{2i} - \alpha_i \tilde{W}_i^T W_i \\ &\leq -K_{Z2i} z_{2i}^2 + \varepsilon_M |z_{2i}| - \alpha_i \|\tilde{W}_i\|^2 + \alpha_i \|\tilde{W}_i\| \|W_i\| \end{aligned}$$

$$\begin{aligned}
&= -K_{Z2i} \left(\left(z_{2i} - \frac{\varepsilon_M}{2K_{Z2i}} \right)^2 - \left(\frac{\varepsilon_M}{2K_{Z2i}} \right)^2 \right. \\
&\quad \left. - \frac{\alpha_i}{K_{Z2i}} \left(\frac{\|W_i\|}{2} \right)^2 \right) - \alpha_i \left(\|\tilde{W}_i\| - \frac{\|W_i\|}{2} \right)^2 \\
&= -K_{Z2i} \left(z_{2i} - \frac{\varepsilon_M}{2K_{Z2i}} \right)^2 \text{ or} \left(\left(\|\tilde{W}_i\| - \frac{\|W_i\|}{2} \right)^2 \right. \\
&\quad \left. - \left(\frac{\|W_i\|}{2} \right)^2 - \frac{1}{\alpha_i K_{Z2i}} \left(\frac{\varepsilon_M}{2} \right)^2 \right). \quad (C8)
\end{aligned}$$

\dot{L}_{2i} is negative if

$$\begin{aligned}
\|z_{2i}\| &> \frac{\varepsilon_M}{2K_{Z2i}} + \sqrt{\left(\frac{\varepsilon_M}{2K_{Z2i}} \right)^2 + \frac{\alpha_i}{K_{Z2i}} \left(\frac{\|W_i\|}{2} \right)^2} \\
\text{or} \\
\|\tilde{W}_i\| &> \frac{\|W_i\|}{2} + \sqrt{\left(\frac{\|W_i\|}{2} \right)^2 + \frac{1}{\alpha_i K_{Z2i}} \left(\frac{\varepsilon_M}{2} \right)^2}
\end{aligned}$$

which yield uniform ultimate boundedness of the states $[z_{2i} \ \tilde{W}_{2i}]^T$ with bounds defined above. Note that the bound on z_{2i} can be arbitrarily small by increasing the design gain K_{Z2i} . Similar to proof of Theorem 1 boundedness of the states $[x_{1i} \ z_{1i}]^T$ can be concluded.

APPENDIX D

The Lyapunov function in this case is proposed as

$$L_4 = \left(\sum_{i=1}^{n-1} z_{2i} \right)^2 / \left(2 \sum_{i=1}^{n-1} g_{2i} \right) + \frac{1}{2} \tilde{W}^T \Gamma_i^{-1} \tilde{W} \quad (D1)$$

where $\tilde{W} = \hat{W} - W$. We define the desired control input for system (18) as (D2)

$$\begin{aligned}
u = &-K_{Z2} \bar{H}^T z_2 - \left(\left(\sum_{i=1}^{n-1} f_{3i} \right) / \left(\sum_{i=1}^{n-1} g_{2i} \right) \right) \\
&- \left(\sum_{i=1}^{n-1} \dot{g}_{2i} \times \sum_{i=1}^{n-1} z_{2i} \right) / \left(2 \sum_{i=1}^{n-1} g_{2i} \right)^2 \quad (D2)
\end{aligned}$$

where $\bar{H}_{(n-1) \times 1} = [1 \ \dots \ 1]^T$. However, the desired control input u is a function of unknown dynamics and is approximated by a neural network as $u_1 = -K_{Z2} \bar{H}^T z_2 - (W^T \varphi(\bar{V}^T x) + \varepsilon)$. Taking the derivative of (D1), employing (D2), and choosing the weight update law as (35), we obtain

$$\begin{aligned}
\dot{L}_{2i} = &-K_{Z2} \bar{H}^T z_2^2 - \alpha \tilde{W}^T \tilde{W} + \varepsilon \bar{H}^T z_2 - \alpha \tilde{W}^T W \\
&\leq -K_{Z2} (\bar{H}^T z_2)^2 + \varepsilon_M |\bar{H}^T z_2| \\
&\quad - \alpha \|\tilde{W}\|^2 + \alpha \|\tilde{W}\| \|W\|. \quad (D3)
\end{aligned}$$

Similar to (C8) \dot{L}_4 is negative if

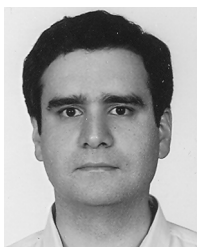
$$\begin{aligned}
|\bar{H}^T z_2| &> \frac{\varepsilon_M}{2K_{Z2}} + \sqrt{\left(\frac{\varepsilon_M}{2K_{Z2}} \right)^2 + \frac{\alpha}{K_{Z2}} \left(\frac{\|W\|}{2} \right)^2} \\
\text{or} \\
\|\tilde{W}\| &> \frac{\|W\|}{2} + \sqrt{\left(\frac{\|W\|}{2} \right)^2 + \frac{1}{\alpha K_{Z2}} \left(\frac{\varepsilon_M}{2} \right)^2}
\end{aligned}$$

which yield uniform ultimate boundedness of $\bar{H}^T z_2$ with bounds defined.

REFERENCES

- [1] P. Kundur, J. Paserba, V. Ajjarapu, G. Andersson, A. Bose, C. Canizares, N. Hatzargyriou, D. Hill, A. Stankovic, C. Taylor, V. T. Cutsem, and V. Vittal, "Definition and classification of power system stability IEEE/CIGRE joint task force on stability terms and definitions," *IEEE Trans. Power Syst.*, vol. 19, no. 3, pp. 1387–1401, Aug. 2004.
- [2] C. Li-Jun and I. Erlich, "Simultaneous coordinated tuning of PSS and FACTS damping controllers in large power systems," *IEEE Trans. Power Syst.*, vol. 20, no. 1, pp. 294–300, Feb. 2005.
- [3] H. Wang, "A unified model for the analysis of FACTS devices in damping power system oscillations—Part III: Unified power flow controller," *IEEE Trans. Power Del.*, vol. 15, no. 3, pp. 978–983, Jul. 2000.
- [4] B. C. Pal, "Robust damping of interarea oscillations with unified power-flow controller," *Proc. Inst. Elect. Eng., Gen., Transm., Distrib.*, vol. 149, no. 6, pp. 733–738, Nov. 2002.
- [5] N. Yang, Q. Liu, and J. D. McCalley, "TCSC controller design for damping interarea oscillations," *IEEE Trans. Power Syst.*, vol. 13, no. 4, pp. 1304–1310, Nov. 1998.
- [6] J. Guo, "Decentralized control and placement of multiple unified power flow controllers," Ph.D. dissertation, Missouri Univ. Sci. Technol., Rolla, MO, 2006, pp. 40–67.
- [7] E. Ghollipour and S. Saadat, "Improving transient stability of power systems using UPFC," *IEEE Trans. Power Del.*, vol. 20, no. 2, pp. 1677–1682, Apr. 2005.
- [8] U. Gabrijel and R. Mihalic, "Direct methods for transient stability assessment in power systems comprising controllable series devices," *IEEE Trans. Power Syst.*, vol. 17, no. 4, pp. 1116–1122, Nov. 2002.
- [9] N. Tambey and M. L. Kothari, "Damping of power system oscillations with unified power flow controller (UPFC)," *Proc. Inst. Elect. Eng., Gen., Transm., Distrib.*, vol. 150, no. 2, pp. 129–140, Mar. 2003.
- [10] M. Januszewski, J. Machowski, and J. W. Bialek, "Application of direct Lyapunov method to improve damping of power swings by control of UPFC," *Proc. Inst. Elect. Eng., Gen., Transm., Distrib.*, vol. 151, no. 2, pp. 252–260, Mar. 2004.
- [11] J. J. Ford, G. Ledwich, and Z. Y. Dong, "Nonlinear control of single-machine-infinite-bus transient stability," in *Proc. IEEE Power Eng. Soc. General Meeting*, Jun. 18–22, 2006.
- [12] M. Poshtan, B. N. Singh, and P. Rastgoufard, "A nonlinear control method for SSSC to improve power system stability," in *Proc. Int. Conf. Power Electronics, Drives and Energy Systems*, Dec. 12–15, 2006, pp. 1–7.
- [13] M. A. Pai, *Energy Function Analysis of Power Systems*. Norwell, MA: Kluwer International Series, 1989.
- [14] M. Ghandhari, G. Anderson, and I. A. Hiskens, "Control Lyapunov functions for controllable series devices," *IEEE Trans. Power Syst.*, vol. 16, no. 4, pp. 689–694, Nov. 2001.
- [15] V. Azbe, U. Gabrijel, D. Povh, and R. Mihalic, "The energy function of a general multi machine system with a unified power flow controller," *IEEE Trans. Power Syst.*, vol. 20, no. 3, pp. 1478–1485, Aug. 2005.
- [16] M. Noroozian, M. Ghandhari, G. Andersson, J. Gronquist, and I. Hiskens, "A robust control strategy for shunt and series reactive compensators to damp electromechanical oscillations," *IEEE Trans. Power Del.*, vol. 16, no. 4, pp. 812–817, Oct. 2001.
- [17] Y. Guo, D. Hill, and Y. Wang, "Nonlinear decentralized control of large-scale power systems," *Automatica*, vol. 36, pp. 1275–1289, 2000.
- [18] M. Noroozian, L. Angquist, M. Ghandhari, and G. Anderson, "Use of UPFC for optimal power flow control," *IEEE Trans. Power Del.*, vol. 12, no. 4, pp. 1629–1634, Oct. 1997.

- [19] K. Mekki, N. M. Hadjsaid, D. Georges, and R. Feuillet, "LMI versus non-linear techniques for the design of FACTS controller," in *Proc. IEEE Power Eng. Soc. Winter Meeting*, Jan. 2002, vol. 2, pp. 1501–1505.
- [20] F. L. Lewis, S. Jagannathan, and A. Yesildirek, *Neural Network Control of Robot Manipulators and Nonlinear Systems*. New York: Taylor & Francis, 1999.
- [21] B. Igel'nik and Y. H. Pao, "Stochastic choice of basis functions in adaptive function approximation and the functional-link net," *IEEE Trans. Neural Netw.*, vol. 6, no. 6, pp. 1320–1329, Nov. 1995.
- [22] V. Azbe and R. Mihalic, "The control strategy for an IPFC based on the energy function," *IEEE Trans. Power Syst.*, vol. 23, no. 4, pp. 1662–1669, Nov. 2008.



Shahab Mehraeen (S'08) received the B.S. degree in electrical engineering from Iran University of Science and Technology, Tehran, Iran, in 1995, the M.S. degree in electrical engineering from Esfahan University of Technology, Esfahan, Iran, in 2001, and the Ph.D. degree in electrical engineering from Missouri University of Science and Technology, Rolla, in 2009.

He is currently a postdoctoral fellow in the Missouri University of Science and Technology. His research interests include renewable energies, power system control, decentralized control of large-scale interconnected systems, and nonlinear, adaptive, and optimal control of dynamical systems.



S. Jagannathan (M'89–SM'99) received the B.S. degree in electrical engineering from College of Engineering, Guindy at Anna University, Madras, India, in 1987, the M.S. degree in electrical engineering from the University of Saskatchewan, Saskatoon, SK, Canada, in 1989, and the Ph.D. degree in electrical engineering from the University of Texas, Austin, in 1994.

During 1986 to 1987, he was a junior engineer at Engineers India Limited, New Delhi, as a Research Associate and Instructor from 1990 to 1991, at the University of Manitoba, Winnipeg, MB, Canada, and worked at Systems and Controls Research Division, Caterpillar, Inc., Peoria, IL, as a consultant during 1994 to 1998. During 1998 to 2001, he was at the University of Texas at San Antonio, and since September 2001, he has been at the University of Missouri, Rolla, where he is currently a Rutledge-Emerson Distinguished Professor and Site Director for the NSF Industry/University Cooperative Research Center on Intelligent Maintenance Systems. He has coauthored over 78 peer reviewed journal articles, 150 IEEE conference articles, several book chapters, and three books entitled *Neural Network Control of Robot Manipulators and Nonlinear Systems* (London, U.K.: Taylor & Francis, 1999), *Discrete-Time Neural Network Control of Nonlinear Discrete-Time Systems* (Boca Raton, FL: CRC, 2006), and *Wireless Ad Hoc and Sensor Networks: Performance, Protocols and Control* (Boca Raton, FL: CRC, 2007). He holds 17 patents with several pending. His research interests include adaptive and neural network control, computer/communication/sensor networks, prognostics, and autonomous systems/robotics.

Prof. Jagannathan received NSF Career Award in 2000, Caterpillar Research Excellence Award in 2001, Boeing Pride Achievement Award in 2007, and many others. He served as an Associate Editor for the IEEE TRANSACTIONS ON NEURAL NETWORKS, IEEE TRANSACTIONS ON CONTROL SYSTEMS TECHNOLOGY, and IEEE SYSTEMS JOURNAL. He served on a number of IEEE Conference Committees.



Mariesa L. Crow (M'80–SM'94–F'10) received the B.S.E. degree from the University of Michigan, Ann Arbor, and the Ph.D. degree from the University of Illinois, Chicago.

She is presently the Director of the Energy Research and Development Center and the F. Finley Distinguished Professor of Electrical Engineering at the Missouri University of Science and Technology, Rolla. Her research interests include developing computational methods for dynamic security assessment and the application of power electronics in

bulk power systems.